Sensitivity Study of ATF Loaded APR1400 Core based on Cr Coating Thickness

Kibeom Park*, Tongkyu Park, Sung-Kyun Zee
FNC Tech., 46 Tapsil-ro, Giheung-gu, Yongin-si, Gyeonggi-do, 17084, Republic of Korea
**Corresponding author: kpark1026@fnctech.com*

1. Introduction

There have been active studies on developing accident tolerant fuel (ATF) since the Fukushima disaster in 2011 [1,2]. One of the primary concepts of ATF is to replace traditional cladding made of Zr-based alloy (so-called "Zircaloy") with SiC-based materials. Another promising concept is the chromium coated zirconium based alloy cladding ATF (Cr-coated ATF) [3]. The preliminary difference between current nuclear fuel [4] and ATFs in terms of assembly depletion [5] was demonstrated in a previous paper.

This study used nTRACER to examine the impact of Cr coating thickness in the 2D APR1400 core [6]. Multiplication factor (k-eff), MTC, and burnup calculations were carried out, and the results were examined, in order to compare the impact of Cr-coat thickness.

2. Methodology

2.1 APR1400 2D Core

Fig. 1 shows the APR1400 core's 2D configuration [4]. There were three types of assemblies for different Uranium enrichment. Since it is a 2D core, the effect along the axial direction is not taken into account. To improve the reliability of the comparison, the 2D core model was made as close to the specific shape and material of the fuel pin, fuel assembly, barrel, reflector, assembly gap, and so on as possible.

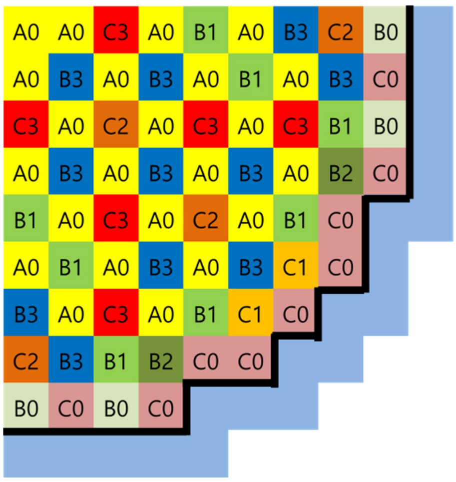

Fig. 1. APR1400 2D core configuration.

2.2 Sensitivity Study of Cr Coating Thickness

As shown in Fig. 2, Cr-coated fuel rods are manufactured by applying a thin Cr coating to the existing Zircaloy cladding. For the sensitivity study, the thickness of the Cr-coat was taken into account differently. The considered thicknesses were 13, 15, 17 and 20 μm.

Additionally, because the results of the analysis may differ depending on the temperature condition or soluble boron concentration of the core, sensitivity calculations were performed under CZP, HZP, HFP, and different soluble boron concentration conditions, respectively.

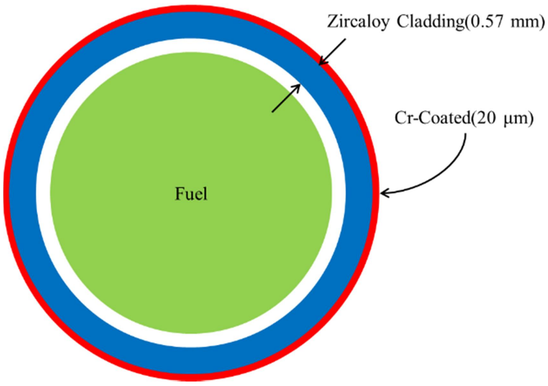

Fig. 2. Schematic of Cr-coated fuel rod.

Table I shows the calculation cases considered in the sensitivity study.

Table I. Sensitivity Study Cases with Different Thickness

SB Conc.	0 ppm			1000 ppm			2000 ppm		
Temp. Condition	CZ	HZ	HF	CZ	HZ	HF	CZ	HZ	HF
k-eff	O	O	O	O	O	O	O	O	O
Power Distribibution.	O	O	O	O	O	O	O	O	O
MTC	X	X	X	O	O	O	X	X	X
Burnup	HFP Depletion Calculation (Critical Boron Search)								

3. Calculation Results and Assessments

The sensitivity calculation was performed in accordance with Table I. The ray condition for nTRACER calculation is set to 0.05/16/4 (Ray Spacing/Azimuthal Angle/Polar Angle).

3.1 k-eff & Power Distribution

First, steady-state calculations for various temperatures and soluble boron conditions were performed. difference between 13 µm and base condition, which is the current fuel rod only without ATF is shown in Table II. Tables III~V show the other results from 15 to 20 µm.

Table II. Reactivity Difference between 13 µm and Base

Category	0 ppm	1000 ppm	2000 ppm
CZP (pcm)	465	275	179
HZP (pcm)	482	335	242
HFP (pcm)	194	332	241

Table III. Reactivity Difference between 15 µm and Base

Category	0 ppm	1000 ppm	2000 ppm
CZP (pcm)	537	318	206
HZP (pcm)	556	386	279
HFP (pcm)	268	383	278

Table IV. Reactivity Difference between 17 µm and Base

Category	0 ppm	1000 ppm	2000 ppm
CZP (pcm)	608	360	234
HZP (pcm)	630	437	317
HFP (pcm)	341	434	316

Table V. Reactivity Difference between 20 µm and Base

Category	0 ppm	1000 ppm	2000 ppm
CZP (pcm)	715	423	274
HZP (pcm)	741	514	373
HFP (pcm)	451	511	371

In the case of power distribution, the effect of the Cr-coat thickness was most strongly related to the error. Figures 3~6 depict the power distribution error for each thickness. The HFP, 1000 ppm, was used as the calculation condition in Fig. 3.

1.16	1.04	0.74	0.71	0.44	0.30	-0.14	-0.53	-0.59
1.04	0.86	0.82	0.57	0.50	0.18	-0.03	-0.48	-0.59
0.74	0.82	0.59	0.58	0.30	0.20	-0.21	-0.48	-0.55
0.71	0.57	0.58	0.35	0.30	-0.01	-0.14	-0.45	-0.55
0.44	0.50	0.30	0.30	0.01	-0.06	-0.38	-0.51	
0.30	0.18	0.20	-0.01	-0.06	-0.40	-0.58	-0.59	
-0.14	-0.03	-0.20	-0.14	-0.38	-0.58	-0.63		
-0.53	-0.49	-0.47	-0.45	-0.51				
-0.58	-0.59	-0.54	-0.56					

Fig. 3. Power distribution error, 13 µm.

1.35	1.21	0.86	0.83	0.51	0.35	-0.17	-0.62	-0.68
1.21	1.00	0.96	0.66	0.59	0.21	-0.04	-0.56	-0.69
0.86	0.96	0.69	0.68	0.35	0.24	-0.24	-0.56	-0.64
0.83	0.66	0.68	0.41	0.35	-0.01	-0.16	-0.53	-0.64
0.51	0.59	0.35	0.35	0.01	-0.07	-0.44	-0.60	
0.35	0.21	0.24	-0.01	-0.07	-0.46	-0.68	-0.69	
-0.17	-0.04	-0.24	-0.16	-0.44	-0.68	-0.74		
-0.62	-0.57	-0.55	-0.53	-0.60				
-0.68	-0.69	-0.64	-0.65					

Fig. 4. Power distribution error, 15 µm.

1.74	1.56	1.11	1.06	0.66	0.45	-0.21	-0.79	-0.88
1.56	1.29	1.23	0.85	0.75	0.27	-0.05	-0.72	-0.88
1.11	1.23	0.89	0.87	0.45	0.31	-0.31	-0.71	-0.83
1.06	0.85	0.87	0.53	0.45	-0.01	-0.20	-0.68	-0.83
0.66	0.75	0.45	0.45	0.02	-0.09	-0.57	-0.77	
0.45	0.27	0.31	-0.01	-0.09	-0.59	-0.87	-0.89	
-0.21	-0.05	-0.30	-0.20	-0.57	-0.87	-0.95		
-0.79	-0.73	-0.71	-0.68	-0.77				
-0.87	-0.88	-0.82	-0.84					

Fig. 5. Power distribution error, 17 µm.

1.93	1.73	1.23	1.18	0.73	0.50	-0.24	-0.88	-0.98
1.73	1.43	1.37	0.95	0.84	0.30	-0.05	-0.80	-0.98
1.23	1.37	0.99	0.97	0.50	0.34	-0.35	-0.79	-0.92
1.18	0.95	0.97	0.59	0.50	-0.01	-0.23	-0.76	-0.92
0.73	0.84	0.50	0.50	0.02	-0.10	-0.63	-0.86	
0.50	0.30	0.34	-0.01	-0.10	-0.66	-0.97	-0.99	
-0.24	-0.05	-0.34	-0.23	-0.63	-0.97	-1.06		
-0.88	-0.81	-0.78	-0.76	-0.86				
-0.97	-0.98	-0.91	-0.93					

Fig. 6. Power distribution error, 20 µm.

3.2 MTC

In the next step, a different temperature condition was used to obtain the MTC. For each condition, the difference in base temperature was 5K. Table VI shows the MTC values for each power condition. The thickness made no discernible difference.

Table VI. MTC for each Cr-coat thickness

Category	CZP	HZP	HFP
13 µm	-0.06	-1.19	-1.25
15 µm	-0.06	-1.19	-1.25
17 µm	-0.06	-1.21	-1.25
20 µm	-0.06	-1.20	-1.26

* MTC, pcm/K

3.3 Depletion Calculation

Finally, the burnup effect was compared for each burnup step, as well as the cycle length at EOC. The difference and relative difference between the base condition and the others is shown in Table VII. The cycle length was slightly reduced as a result of the Cr-coat thickness.

Table VII. Cycle Length for each Cr-coat thickness

Category	13 µm	15 µm	17 µm	20 µm
Cycle Length	-9 (-2.0%)	-11 (-2.3%)	-12 (-2.6)	-14 (-3.1%)

* Cycle Length, days

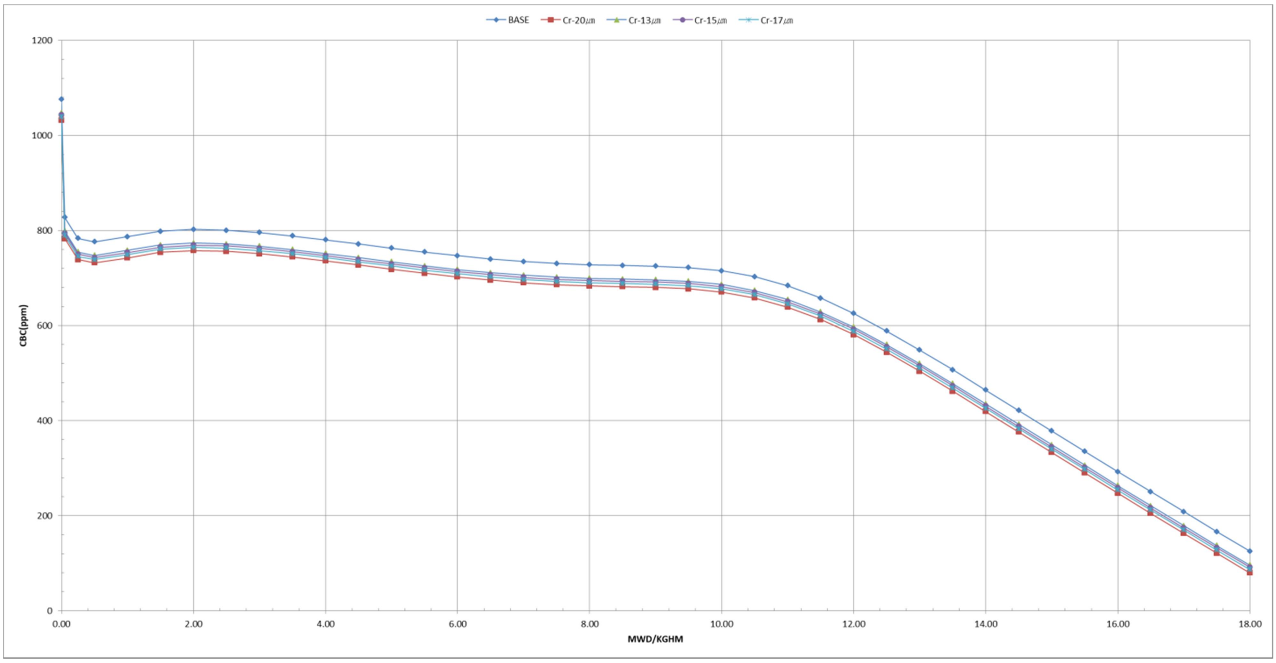

Fig. 7. Burnup effect comparison results for each Cr-coat thickness.

4. Conclusion

For the 2D APR 1400 core, sensitivity calculations were performed for each Cr-coat thickness. The comparison of the values k-eff, power distribution, MTC, and cycle length confirmed that the ATF had no effect on the core.

ACKNOWLEDGEMENT

This work was supported by the Nuclear Safety Research Program through the Korea Foundation Of Nuclear Safety (KoFONS) using the financial resource granted by the Nuclear Safety and Security Commission (NSSC) of the Republic of Korea. (No. 2103051)

REFERENCES

[1] H. Rho, Y. Lee, Development of a 2D axisymmetric SiC cladding mechanical model and its applications for steady-state and LBLOCA analysis, Journals of Nuclear Materials, Vol. 558, 2022.

[2] Y. Lee, T. J. McKrell, C. Yue, M.S. Kazimi, Safety assessment of SiC cladding oxidation under loss-of-coolant accident conditions in light water reactors, Nucl. Technol. 183 (2), 210–227, 2013.

[3] KNF, 사고저항성 핵연료 개발 현황 및 연소시험 계획, 2019 안전해석 심포지엄 자료집, 2019.

[4] S. Yuk, DeCART Solutions of APR1400 Reactor Core Benchmark Problems, Transactions of the Korea Nuclear Society Virtual Autumn Meeting, 2019.

[5] K. Park, T. K. Park, S. K. Zee, Preliminary Analysis of Burnup Effect on k-inf for Cr-Coated and SiC Cladding Accident Tolerant Fuel Rods with nTRACER, Transactions of the Korea Nuclear Society Spring Meeting, Jeju, R.O.Korea, May 19-20, 2022.

[6] M. Ryu, Y. S. Jung, H. H. Cho, H. G. Joo, Solution of the BEAVRS benchmark using the nTRACER direct whole core calculation code, Journals of Nuclear Science and Technology, Vol. 52, Issue 7-8, pp. 961-969, 2015.